

Sub-word Level Lip Reading With Visual Attention

Prajwal K R Triantafyllos Afouras Andrew Zisserman
Visual Geometry Group, University of Oxford
{prajwal, afouras, az}@robots.ox.ac.uk

Abstract

The goal of this paper is to learn strong lip reading models that can recognise speech in silent videos. Most prior works deal with the open-set visual speech recognition problem by adapting existing automatic speech recognition techniques on top of trivially pooled visual features. Instead, in this paper we focus on the unique challenges encountered in lip reading and propose tailored solutions. To that end we make the following contributions: (1) we propose an attention-based pooling mechanism to aggregate visual speech representations; (2) we use sub-word units for lip reading for the first time and show that this allows us to better model the ambiguities of the task; (3) we propose a training pipeline that balances the lip reading performance with other key factors such as data and compute efficiency. Following the above, we obtain state-of-the-art results on the challenging LRS2 and LRS3 benchmarks when training on public datasets, and even surpass models trained on large-scale industrial datasets by using an order of magnitude less data. Our best model achieves 22.6% word error rate on the LRS2 dataset, a performance unprecedented for lip reading models, significantly reducing the performance gap between lip reading and automatic speech recognition.

1. INTRODUCTION

Lip reading, or visual speech recognition, is the task of recognising speech from silent video. It has many practical applications which include improving speech recognition in noisy environments, enabling silent dictation, or dubbing and transcribing archival silent films [21]. It also has important medical applications, such as helping speech impaired individuals, e.g. people suffering from Lou Gehrig’s disease speak [41], or enabling people with aphonia (loss of voice) to communicate just by using lip movements.

Lip reading and audio-based automatic speech recognition (ASR) both have the common goal of transcribing speech, however they differ regarding the input: while in ASR the input signal is an audio waveform, in essence a

one-dimensional time-series, lip reading has to deal with high-dimensional video inputs that have both temporal and spatial complexity. This added complexity makes training large end-to-end models harder due to GPU memory and computation constraints. Furthermore, understanding speech from visual information alone is challenging due to inherent ambiguities present in the visual stream, i.e. the existence of homophemes, different characters that are visually indistinguishable (e.g. ‘pa’, ‘ba’ and ‘ma’). That lip reading is a much harder task is also supported by the fact that although humans can understand speech reasonably well even in the presence of noise and through a variety of accents, they perform relatively poorly on lip reading [5, 12].

Designing a lip reading model requires both a visual component – mouth movements need to be identified – as well as a temporal sequence modelling component, which typically involves learning a language model that can resolve ambiguities in individual lip shapes. Recent developments in deep learning models and the availability of large scale annotated datasets has led to breakthroughs, surpassing human performance [12]. However, most of these works have taken the approach of adapting techniques used for ASR and machine translation, without catering to the particularities of the vision problem.

The conjecture in this paper is that the performance of lip reading, in terms of both accuracy and data efficiency, can be improved if the model is designed from the start taking account of the peculiarities of the visual, rather than the audio domain. To this end, we make four contributions to this design.

Visual encoding. Our first contribution is the design of a novel visual backbone for lip reading. The spatio-temporal complexity in lip reading requires dealing with problems such as tracking the mouth in moving talking heads. This is usually achieved with complicated pre-processing pipelines based on facial landmarks. However, those are sub-optimal in many cases. For example, landmarks don’t work well in profile views [22]. Moreover, it is unclear what is the optimal region-of-interest for lip reading: it has been shown that besides the lips, other parts of the face, e.g. the cheeks, may

also contain useful discriminative information [52]. Also, this region-of-interest can vary drastically in terms of scale, aspect ratio across identities and utterances. Thus, in this work, we propose an end-to-end trainable attention-based pooling mechanism that learns to track and aggregate the lip movement representations, resulting in a significant performance boost.

Text tokenisation. Lip reading methods most commonly output character-level tokens. This output representation however is sub-optimal as characters are more fine-grained than the input, with multiple characters corresponding to a single video frame. Furthermore, characters do not encode any prior knowledge about the language, leading to higher dependence on external language models which must also ‘learn to read’. In this work we instead use sub-word tokens (word-pieces) which not only match with multiple adjacent frames but are also semantically meaningful for learning a language easily. Word-pieces result in much shorter (than character) output sequences which greatly reduces the runtime and memory requirements. They also provide a language prior, reducing the language modelling burden of the model. We experimentally compare character and word-piece tokenization to justify this choice.

Training curriculum. Curriculum learning has been used in both ASR and lip reading as a way to accelerate model convergence and improve final performance. Prior lip reading works are often trained in two stages [1, 12]: First the visual backbone is pre-trained on a limited context lip reading task (e.g. word-level recognition); the backbone is then frozen and a new sequence model is trained on top of it on a sentence-level task. The second stage follows a curriculum [1, 12] that gradually increases the length of the sentences, a practice that has its roots in audio sequence modelling [8]. Among other findings in this work, we show that (i) it is possible to skip word-level lipreading and pre-train the backbone directly on the sentence transcription task, albeit keeping the sentences to a manageable level, e.g. 2 words, and (ii) it is possible to do away with the complicated curriculum that gradually increases the sentence length by simply sub-sampling word sequences as a form of augmentation.

Besides improving performance on the sentence-level lip reading task itself, obtaining improved lip movement representations can have broader impact, as those are often used for other related downstream tasks – e.g. sound source separation [16], visual keyword spotting [34], and visual language identification [4]. Moreover the temporal augmentation we propose can be extended to other visual speech translation tasks, such as sign language recognition [43].

In summary, we make the following four contributions and show their benefits to improving lip reading performance: (i) a visual backbone architecture using attention based pooling on the spatial feature map; (ii) the use of

sub-word units, rather than characters for the language tokens; and (iii) a two stage curriculum training schedule that simplifies the training process, without a significant performance cost.

As will be seen, with these design choices and training methodology, the performance of our best models exceeds prior work on standard evaluation benchmarks, and even outperforms proprietary models that use an order of magnitude more data for training.

2. Related Work

We present an overview of prior work on lip reading, including a discussion of how these methods select and track the visual regions of interest, as well as the output tokenizations they use, followed by a brief overview of temporal augmentations and the use of attention for visual feature aggregation in other domains.

2.1. Lip reading

Early works on lip reading relied on hand-crafted pipelines and statistical models for visual feature extraction and temporal modelling [18, 29, 35, 36, 39]; an extensive review of those methods is presented in [54]. The advent of deep learning and the availability of large scale lip reading datasets such as LRS2 [11] and LRS3 [2], rejuvenated this area. Progress was initially on word level recognition [12, 42], and then moved onto sentence level recognition by adapting models developed for ASR using LSTM sequence-to-sequence [11] or CTC [5, 41] approaches. [38] take a hybrid approach, training an LSTM-based sequence-to-sequence model with an auxiliary CTC loss. One trend in recent work is moving to Transformer based architectures [1], or variants using convolution blocks [51], and hybrid architectures like a Conformer [19]. Another trend is to investigate the benefits of training with larger datasets, either directly by training on proprietary data that is orders of magnitude larger than any public dataset [32], or indirectly by distilling ASR models into lip reading ones [3, 28, 49]. For visual feature extraction and short-term dynamic modelling, most modern pipelines rely on spatio-temporal CNNs consisting of multiple 3D convolutional layers [5, 41], or more lightweight alternatives that comprise a single 3D convolutional layer followed by 2D ones [1, 12, 42] applied frame-wise.

2.2. Mouth ROI selection, registration and tracking

A thorough investigation on facial region of interest (ROI) selection for lip reading is provided by [52]. The videos included in datasets like LRS2 and LRS3 are commonly pre-processed with a face detection and tracking pipeline which outputs clips roughly centered around the speaker’s face. Many previous works use a central crop

on the provided videos as input to the feature extractors [1, 30, 42]. More elaborate pipelines use facial landmarks to register the face to a canonical view and/or only extract the crops of the mouth area [5, 27, 32, 37, 41, 51]. [52] propose inputting a large part of the face, combined with Cutout [14] to encourage the model to also use the extra-oral face regions. After selecting which input region to extract the low-level CNN features from, all above works apply Global Average Pooling (GAP) on the extracted visual features map; this obtains a compact representation, but discards spatial information. Recent works [51] have shown that replacing GAP with a Spatio-temporal fusion module improves performance.

2.3. Text tokenization

Most prior works on lip reading output character-level predictions [1, 10, 11, 30, 32, 38, 51]. Those approaches usually use an external language model during inference to boost performance [23, 31]. Instead [41] chose to output phoneme sequences, using phonetic dictionaries. This approach has the advantage of a more accurate mapping of lip-movements to sounds, but requires a complicated decoding pipeline involving a proprietary finite-state-transducer. [17, 26] use a hard-crafted heuristic to map words onto viseme sequences and vice versa, and use viseme tokens for representing the output and target text. In this work we instead propose using sub-word level tokenisation, which greatly reduces the output sequence length, thus accelerating both training and inference, and neatly encodes prior language information improving overall performance.

2.4. Visual feature aggregation with attention

Our work is also related to methods that use attention for improving visual representations of images or videos. [20, 45] use attention-weighted-averages of visual features as building blocks for various classification and detection tasks, while OCNNet [50] uses self-attention to model context between pixels for semantic segmentation. A number of recent papers has replaced convolutions with Transformer [44] blocks in visual representation pipelines. DETR [7] and efficient DETR [48] learn object detectors by applying spatial transformers on top of CNN feature extractors. Similarly, the Visual Transformer [46] tokenises low-level CNN features and then processes them using a Transformer to model relationships between tokens. ViT [15] completely removes CNNs from the visual pipeline, replacing them with Transformer layers applied on image patch sequences, while the Timesformer [6] has been suggested as a purely Transformer-based solution for video representation learning.

3. Method

In this section we describe our proposed method. The architecture of the model is outlined in Figure 1.

3.1. Visual backbone

3.1.1 CNN

The input to the pipeline is a silent video clip of T frames, $\mathbf{x} \in \mathcal{R}^{T \times H \times W \times 3}$. A spatio-temporal residual CNN is applied on sub-clips of 5 frames (i.e. 0.2s) with a unit frame stride, to extract visual spatial feature maps $\mathbf{f} \in \mathcal{R}^{T \times h \times w \times c}$. For our best model, $H = W = 96$, $(h, w) = (H/4, W/4) = (28, 28)$, and $c = 128$.

3.1.2 Visual Transformer Pooling

The CNN feature map $\mathbf{f}_t \in \mathcal{R}^{h \times w \times c}$ corresponding to every input frame $t \in \{1, \dots, T\}$ is processed individually by a shared Visual Transformer Pooling (VTP) block. The feature map is first flattened to $\mathbf{f}_t \in \mathcal{R}^{h \times w \times c}$ and projected to a desired Transformer feature dimension d to get $\mathbf{f}_t \in \mathcal{R}^{hw \times d}$. Then, spatial positional encodings (SPE) are added to it; the result is passed through an encoder consisting of N_{VTP} Transformer layers, to produce an enhanced self-attended feature map

$$\mathbf{z}_t = \text{encoder}_v(\mathbf{f}_t + \text{SPE}_{1:hw}) \in \mathcal{R}^{hw \times d}.$$

A learnable query vector $\mathbf{Q}_{att} \in \mathcal{R}^{d \times 1}$ is then used to extract a visual attention mask

$$\mathbf{a}_t = \text{softmax}(\mathbf{Q}_{att}^\top \mathbf{z}_t) \in \mathcal{R}^{hw \times 1}.$$

The attention mask is used to compute a weighted average over the self-attended feature map

$$\mathbf{g}_t = \frac{1}{hw} \sum_{u=1}^{hw} \mathbf{a}_t^u \mathbf{z}_t^u \in \mathcal{R}^d$$

where \mathbf{a}_t^u and \mathbf{z}_t^u denote the feature and attention weight respectively, associated with frame t and location $u \in \{1, \dots, hw\}$. By stacking the resulting vectors \mathbf{g}_t in time, we obtain an embedding sequence $\mathbf{g} = (\mathbf{g}_1, \mathbf{g}_2 \dots, \mathbf{g}_T) \in \mathcal{R}^{T \times d}$ which contains a compact spatio-temporal representation for every input frame.

3.1.3 Transformer encoder-decoder

An encoder-decoder Transformer model is used to predict a text token sequence $s = (s_1, s_2 \dots, s_{T_{dec}})$ from the source video embedding sequence \mathbf{g} , one token at a time: temporal positional encodings (PE) are added to \mathbf{g} , and the result is input to an encoder, which consists of N_{enc} multi-head

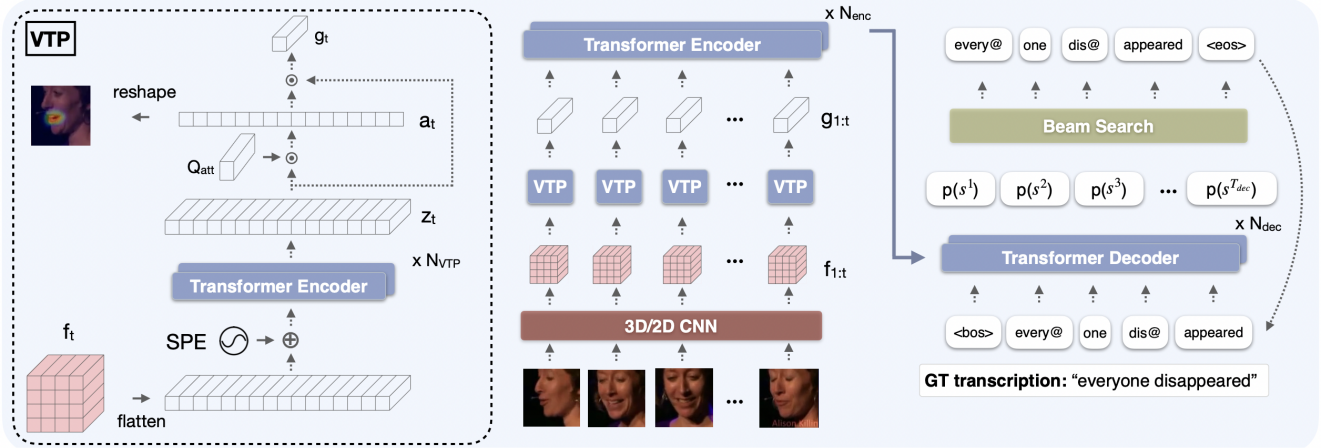


Figure 1. **Proposed lip reading architecture.** *Left:* The input video frames are passed through a spatio-temporal CNN to extract low-level visual features \mathbf{f} . The feature map corresponding to every input frame is then separately processed by a Visual Transformer Pooling module (VTP). The VTP block adds spatial positional encodings (SPE) to the input features and passes the result through a Transformer encoder to produce a self-attended feature map \mathbf{z}_t . A query vector \mathbf{Q}_{att} is used to compute an attention mask which is in turn used to obtain a spatially weighted average of \mathbf{z}_t . This produces a compact visual representation of the appearance and lip movement around each input video frame. Concatenating the frame-wise features forms a temporal feature sequence \mathbf{g} . This is passed as input to an encoder-decoder Transformer (*right*) that auto-regressively predicts sub-word probabilities for one token at a time. An output sentence is eventually inferred from these distributions using a beam search.

Transformer layers, to produce a self-attended embedding sequence

$$\mathbf{g}_{enc} = \text{encoder}(\mathbf{g} + PE_{1:T}) \in \mathcal{R}^{T \times d}.$$

The decoder, which consists of N_{dec} Transformer layers, then attends on this sequence and predicts the output text token sequence s in an auto-regressive manner, by factorising its joint probability:

$$\log p(s|\mathbf{x}) = \sum_{t=1}^{T_{dec}} \log p(s_t | \mathbf{g}_{enc}(\mathbf{x}), s_{1:t-1}) \quad (1)$$

where positional encodings have also been added to the auto-regressive decoder inputs as in [44].

The text sentences are encoded into token sequences (and vice versa tokens are decoded into text) using a sub-word level tokeniser, in particular WordPiece [47]. We tried other sub-word tokenizations such as Byte-Pair-Encoding (BPE) that is used in GPT2 [40], but it performed worse compared to using WordPiece.

3.1.4 Beam search decoding and rescoreing

Decoding is performed with a left-to-right beam search of width B . We also decode a second time after flipping all the input video frames horizontally. Additional language knowledge can be incorporated by using an external language model (LM) to re-score [9] the $2 \times B$ -best hypotheses $S = \{s_1 \cdots s_B; s_1^h \cdots s_B^h\}$ that the beam searches result

in, and obtain the highest scoring one as the final sentence prediction:

$$s_{best} = \arg \max_{s \in S} [\alpha \log p(s|\mathbf{x}) + (1 - \alpha) \log p_{LM}(s)]$$

Here, $s_1^h \cdots s_B^h$ denotes the beam sequences after horizontally flipping the input. We found that additional test-time augmentations such as small degrees of rotation and/or color jitters did not improve the results.

3.2. Training

3.2.1 Optimisation objective

Given a training dataset \mathcal{D} consisting of pairs (x, s^*) of video clips and their ground truth transcriptions, the model is trained to maximise the log likelihoods of the transcriptions by optimising the following objective

$$\mathcal{L} = -\mathbb{E}_{(x, s^*) \in \mathcal{D}} \log p(s^*|\mathbf{x}) \quad (2)$$

3.2.2 Teacher forcing

To accelerate training we follow common practice for sequence-to-sequence training with Transformers, and feed in the previous ground truth token as the decoder input at every step, instead of using auto-regression. The tokens are fed into the decoder via a learnable embedding layer.

3.2.3 Training protocol

Training is performed in two stages. First the whole network is trained end-to-end on short sentences of 2 words. Following [1, 12] we use frame word-boundaries to crop out training samples from all the possible combinations of 2 consecutive words in the dataset, which provides natural augmentation. Once training converges, we freeze the visual backbone, then pre-extract and dump the visual features of all the samples in the training dataset. In the second training stage that follows, we train the encoder-decoder sub-network on all possible sub-sequences (n-grams) of length 2 or larger that can be generated by combining consecutive word utterances in the dataset.

3.2.4 Discussion

We note that our proposed curriculum is much simpler than the ones commonly used in prior works [1, 12, 38], since (i) the same network and loss are used during the backbone pre-training stage, which provides a good initialization of the entire network and enables a smooth transfer; this is in contrast to other works that pre-train with a different proxy loss and require a separate word classification head which is subsequently discarded; and (ii), the second stage is significantly simpler to implement and requires a single run, unlike curriculums that gradually increase the length of the training sentences and usually require a complicated tuning process with multiple manual restarts to achieve the best results. We observed that our proposed second stage training setup matches the performance of the complicated curriculum strategy, while being more efficient in terms of training time and manual efforts.

4. Experiments

4.1. Data

4.1.1 LRS2 & LRS3

For training and evaluation we use two publicly available sentence-level lip reading datasets: LRS2 [12] and LRS3 [2]. LRS2 contains video clips from a variety of shows from British television, such as Countryfile and Top Gear; the transcribed content sums up to approximately 224 hours in total. LRS3 has been collected from over 5,000 TED and TEDx talks in English, available on YouTube, totalling 475 hours. Both datasets have been created using a detection and tracking pipeline that produces face-cropped clips roughly centered around the speaker’s talking head. All videos are available at a 224×224 pixel resolution and 25 fps. The datasets contain a “pretrain” partition that includes extensive head tracks including word boundaries that have been produced by force-aligning subtitles to the audio. Those word alignments enable training at any granularity.

The test sets contain only full sentences.

4.1.2 Additional dataset: TEDx_{ext}

In order to obtain more training data, we create a new dataset from TEDx talks downloaded from YouTube, by using a pipeline similar to [2]. We collect 13,211 TEDx talks in English that are not included in LRS3. Unlike the videos used for the creation of LRS3 which contain manually annotated transcripts, the new videos only have the closed-captions automatically produced by the YouTube ASR system. As these captions are only approximately aligned to the audio, we use the Montreal Force Aligner [33] to obtain more accurate alignments for the word boundaries needed by our training pipeline (see Section 3.3 of the main paper). For the rest of the processing (face detection, tracking and cropping) we used the same pipeline as in [2]. The resulting training dataset contains 1,204 hours in total over 318,459 visual speech tracks, including text transcriptions with word boundary alignment. We call this new training set TEDx_{ext}. We note that since this pipeline does not require any manual transcriptions, the supervision comes for free, therefore it is easily scalable. However the supervision is not as strong due to the noise in the training data introduced by the imperfect ASR transcriptions. But, as we will see, our model achieves a huge performance boost after training on this noisy data.

4.2. Implementation details

During the first training stage, we apply random visual augmentations on the input frames to reduce overfitting: the input videos are first resized to a square 160 pixels resolution, from which a central square 96-pixel crop is extracted. Random horizontal flipping and rotation are also applied before inputting to the lip reading pipeline. During inference we use the central 96-pixel crop, and only apply the horizontal flipping augmentation.

For our best model, *i.e.*, VTP on $(H/4, W/4)$, we set $N_{VTP} = 6$ layers with 8 heads each for the encoder of the VTP module. For computational efficiency, VTP uses the recently proposed Linear Transformer [24] instead of the original Transformer [44]. We found that this change did not lead to a drop in the recognition performance, while being much more computationally efficient. Another design choice we had to make is deciding after which CNN layer the VTP should be applied. Transformer layers are computationally expensive at higher resolution feature maps (*i.e.* earlier layer activations), but can capture more detailed information. Given this trade-off, we experiment with three different feature map resolutions, at $(h, w) = (H/4, W/4), (H/8, W/8), (H/16, W/16)$. For the latter two variants, we set the feature dimension $d = 512$. When pooling on $(h, w) = (H/4, W/4)$, we keep the

Method	Datasets used	Training	Evaluation	
		Total # hours	LRS2	LRS3
LIBS [53]	LRS2, LRS3	698	65.3	-
Hyb. CTC/Att. [38]	LRS2, LRW	389	63.5	-
TDNN [49]	LRS2	224	48.9	-
Conv-seq2seq [51]	LRS2, LRS3	698	51.7	60.1
CTC + KD [3]	LRS2, LRS3, VoxCeleb2 [‡]	1,032	51.3	59.8
Hyb. + Conformer [30]	LRS2, LRW	389	37.9	-
Hyb. + Conformer [30]	LRS3, LRW	639	-	43.3
Ours	LRS2, LRS3	698	28.9	40.6
TM-seq2seq [1]	LRS2, LRS3, LRW, MV-LRS [†]	1,637	48.3	58.9
CTC-V2P [41]	LSVSR [†]	3,886	-	55.1
RNN-T [32]	YT31k [†]	31,000	-	33.6
Ours	LRS2, LRS3, MV-LRS [†] , TED _x _{ext}	2,676	22.6	30.7

Table 1. Comparison of different lip reading models on the test sets of the LRS2 and LRS3 datasets, including the datasets and the aggregate number of hours used for training each model, in terms of Word Error Rate % (WER, lower is better). Our model achieves state-of-the-art results, outperforming all previous baselines when trained on publicly available data (i.e. LRS2 and LRS3). If we additionally use MV-LRS and TED_x_{ext} for training, then our best model obtains results comparable with those of [32] who train on a very large scale industrial dataset, even though we are only using an order of magnitude less data. This is indicative of the data efficiency of our proposed pipeline. [†]Large non-public labelled datasets: MV-LRS [1] contains 730 hours, LSVSR [41] 3.9k hours, and YT31k [32] 31k hours of transcribed video. [‡]unlabelled dataset. Results shown in blue have been obtained by training (partly or entirely) on non-public data.

Layer	# Channels	Kernel	Stride	Padding	Output dims
input	3	-	-	-	$T \times 96 \times 96$
conv _{1,1}	64	(5,5,5)	(1,2,2)	(2,2,2)	$T \times 48 \times 48$
conv _{2,1}	128	(3,3)	(2,2)	(1,1)	$T \times 24 \times 24$
conv _{2,2}	128	(3,3)	(1,1)	(1,1)	$T \times 24 \times 24$
conv _{2,3}	128	(3,3)	(1,1)	(1,1)	$T \times 24 \times 24$
conv _{3,1}	256	(3,3)	(2,2)	(1,1)	$T \times 12 \times 12$
conv _{3,2}	256	(3,3)	(1,1)	(1,1)	$T \times 12 \times 12$
conv _{3,3}	256	(3,3)	(1,1)	(1,1)	$T \times 12 \times 12$
conv _{4,1}	512	(3,3)	(2,2)	(1,1)	$T \times 6 \times 6$
conv _{4,2}	512	(3,3)	(1,1)	(1,1)	$T \times 6 \times 6$
conv _{4,3}	512	(3,3)	(1,1)	(1,1)	$T \times 6 \times 6$
conv _{5,1}	512	(3,3)	(2,2)	(1,1)	$T \times 3 \times 3$
fc	512	(3,3)	(1,1)	(0,0)	$T \times 1 \times 1$

Table 2. Architecture details for the visual CNN backbone. Batch Normalization and ReLU activation are added after every convolutional layer. Shortcut connections are also added at each layer, except for the first layer of every residual block – i.e. the ones with stride > 1. The layers shown in gray, are only used by the TM-seq2seq baseline and not in our best model.

compute and memory needs in check by performing two small changes: using $d = 256$ for the first 3 VTP layers, and then setting $d = 512$ but down-sampling the feature map to $(H/8, W/8)$ for the remaining 3 layers.

The encoder-decoder Transformer contains $N_{enc} = 6$ and $N_{dec} = 6$ layers with 8 attention heads per layer everywhere. We use sinusoidal positional encodings [44] for PE and learnable positional encodings for SPE. We use the WordPiece tokenizer of the pre-trained BERT model in HuggingFace¹, with a vocabulary of 30522 tokens. We also use an off-the-shelf GPT2 language model for beam rescoring. For the beam rescoring we set hyperparameter $\alpha = 0.7$ for LRS2 and $\alpha = 0.6$ for LRS3 respectively. We train all models with the Adam optimiser [25] with $\beta_1 = 0.9$, $\beta_2 = 0.98$ and $\epsilon = 10^{-9}$. In the first stage of the training we follow a Noam learning rate schedule [44] for the first 50 epochs and then reduce the learning rate by a factor of 5 every time the validation loss plateaus, until reaching 10^{-6} . For the second stage, the learning rate is initially set to $5e^{-5}$ and reduced by a factor of 5 on plateau down to 10^{-6} . For our best reported models on public data, the first stage of training takes approximately 14 days on 4 Tesla v100s GPUs. The second stage takes 1.5 days on 1 Tesla v100 GPU.

4.3. State-of-the-art lipreading

We compare the results of our method to existing works in Table 1. It is clear that our best model outperforms all prior work trained on public data, on both the LRS2 and LRS3 benchmarks. In particular, compared to the strongest baseline of Ma *et al.* [30] our best model performs 9% better

¹https://huggingface.co/transformers/pretrained_models.html



Figure 2. Visualization of the visual attention masks α from the VTP module superimposed on the input frames that produce them. The video clips used here are random samples from the LRS3 dataset. It is evident that the model follows the more discriminative mouth region.

on LRS2 and 2.7% better on LRS3. When also using MV-LRS and TED_{ext} for training, we obtain a significant boost, achieving 22.6% and 30.7% WER for LRS2 and LRS3 respectively. We even outperform [32] by a considerable margin while using $10\times$ lesser training data. This clearly suggests that our pipeline is highly data-efficient.

4.4. Ablations

4.4.1 Importance of each module

We show the impact of each proposed module in the final scores, starting from a variation of the TM-seq2seq model [1]², and building up to our full model. We summarize the results of this study in Table 3. It is clear that all the proposed improvements give significant performance boosts and are largely orthogonal. In particular, the use of WordPiece tokens contributes a 3.8% absolute improvement on LRS2, while introducing the VTP module decreases the WER by 6.3%. Using LM to rescore the beams and applying test-time horizontal flipping contributes to another 1.1% and 0.9% improvement respectively.

4.4.2 VTP resolution

The VTP module is capable of aggregating the spatial features at arbitrary feature map resolutions. But, we show that it is more effective when operating on finer high resolution feature maps rather than coarser low resolution feature maps. This is evident in Table 4, where pooling after $\text{conv}_{2,3}$ at a spatial resolution of 24×24 is much more

²Using the same CNN extractor as our model for fair comparison

Method	WER	Δ
TM-seq2seq [†] baseline	41.0	-
+ WordPiece	37.2	-3.8
+ VTP	30.9	-6.3
+ Beam LM rescoring	29.8	-1.1
+ Test-time augmentation	28.9	-0.9

Table 3. Ablation on the design improvements proposed in this work. The results reported are for the test set of the LRS2 dataset. It is clear that all the proposed components contribute independently to the performance boost. [†] The baseline is an improved version of TM-seq2seq [1] (see Table 2 for details)

effective than pooling on lower-resolution feature maps of 12×12 or 6×6 .

Method	# transformer layers	WER
Without VTP	0	37.2
VTP @ $(H/16, W/16)$	2	35.7
VTP @ $(H/8, W/8)$	3	33.8
VTP @ $(H/4, W/4)$	6	30.9

Table 4. Ablation on the input spatial resolution for the VTP module. The number of Transformer layers for each stage is chosen such that the total number of parameters in the visual front-end is approximately the same. We see that pooling from higher resolution feature maps clearly leads to better results.

4.4.3 Training protocol

Previous works [1] follow a curriculum strategy during training: the sequence length is gradually increased over the course of the training. While this protocol indeed works better, we argue that the boost in performance does not come from the curriculum learning but from something else: data augmentation. Over the course of the training process, the model gets to train on all sub-sequences (n-grams) of various lengths, and this is an effective data augmentation that reduces over-fitting. Indeed, we observe that if we simply train on all n-gram sub-sequences at once (as opposed to slow length increase), we achieve a WER of 30.92, which is comparable to the WER of 30.91 following a curriculum protocol.

Not only does this experiment shed new light on the current understanding of the training pipeline of lip reading, it also achieves similar results while following a much simpler training process that requires significantly less manual tuning.

4.5. Visual attention visualization

In Figure 2 we visualize the visual attention maps that the VTP module produces. Note that the lips region is tracked very accurately while the speakers turn their heads around, even for extreme profile views.

5. Discussion

Narrowing the gap between lip reading and ASR performance opens up opportunities for useful applications, as noted in the introduction, but also raises privacy issues and the risk of potential malign uses. One issue that is often raised is the potential for malign surveillance, e.g. using CCTV footage from public spaces to eavesdrop on private civilian conversations. However, this is in fact very low risk due to a number of factors: we achieve a low WER on benchmarks containing video material that is professionally produced and at high resolutions and frame-rates, with good lighting conditions. Moreover the speakers are aware of being filmed and collaborate, most of the time speaking while frontally facing the camera. In contrast, CCTV usually operate at much lower resolution and frame rates and from unusual angles. As shown in prior work [13, 32, 41], lip reading performance greatly deteriorates with lower frame rate or input resolutions, or when non-frontal (e.g. profile or overhead viewpoints) rather than frontal speaker views are considered.

6. Conclusion

We have presented an improved architecture for lip reading based on attention-based aggregation of visual representations as well as several enhancements of the training

protocol, including temporal augmentations, the use of sub-word output tokenisation, and a more data-efficient learning curriculum. Our best models train and converge faster than other baselines and achieve state-of-the-art results outperforming prior work trained on public data by a significant margin, while also obtaining performance comparable to that of industrial models trained on orders of magnitude more data.

Acknowledgements. Funding for this research is provided by the UK EPSRC CDT in Autonomous Intelligent Machines and Systems, a Google DeepMind Graduate Scholarship, and the EPSRC Programme Grant VisualAI EP/T028572/1.

References

- [1] Triantafyllos Afouras, Joon Son Chung, Andrew Senior, Oriol Vinyals, and Andrew Zisserman. Deep audio-visual speech recognition. *IEEE PAMI*, 2019. 2, 3, 5, 6, 7, 8
- [2] Triantafyllos Afouras, Joon Son Chung, and Andrew Zisserman. LRS3-TED: a large-scale dataset for visual speech recognition. In *arXiv preprint arXiv:1809.00496*, 2018. 2, 5
- [3] Triantafyllos Afouras, Joon Son Chung, and Andrew Zisserman. ASR is all you need: Cross-modal distillation for lip reading. In *International Conference on Acoustics, Speech, and Signal Processing*, 2020. 2, 6
- [4] Triantafyllos Afouras, Joon Son Chung, and Andrew Zisserman. Now you're speaking my language: Visual language identification. In *INTERSPEECH*, 2020. 2
- [5] Yannis M. Assael, Brendan Shillingford, Shimon Whiteson, and Nando de Freitas. Lipnet: Sentence-level lipreading. *arXiv:1611.01599*, 2016. 1, 2, 3
- [6] Gedas Bertasius, Heng Wang, and Lorenzo Torresani. Is space-time attention all you need for video understanding? In *Proc. ICML*, 2021. 3
- [7] Nicolas Carion, Francisco Massa, Gabriel Synnaeve, Nicolas Usunier, Alexander Kirillov, and Sergey Zagoruyko. End-to-end object detection with transformers. In *arXiv preprint arXiv:2005.12872*, 2020. 3
- [8] William Chan, Navdeep Jaitly, Quoc V Le, and Oriol Vinyals. Listen, attend and spell. *arXiv preprint arXiv:1508.01211*, 2015. 2
- [9] William Chan, Navdeep Jaitly, Quoc V. Le, and Oriol Vinyals. Listen, attend and spell: A neural network for large vocabulary conversational speech recognition. In *ICASSP*, 2016. 4
- [10] Joon Son Chung, Arsha Nagrani, and Andrew Zisserman. VoxCeleb2: Deep speaker recognition. In *INTERSPEECH*, 2018. 3
- [11] Joon Son Chung, Andrew Senior, Oriol Vinyals, and Andrew Zisserman. Lip reading sentences in the wild. In *Proc. CVPR*, 2017. 2, 3
- [12] Joon Son Chung and Andrew Zisserman. Lip reading in the wild. In *Proc. ACCV*, 2016. 1, 2, 5

- [13] Joon Son Chung and Andrew Zisserman. Lip reading in profile. In *Proc. BMVC*, 2017. 8
- [14] Terrance DeVries and Graham W. Taylor. Improved regularization of convolutional neural networks with cutout. In *arXiv preprint arXiv:1708.04552*, 2017. 3
- [15] Alexey Dosovitskiy, Lucas Beyer, Alexander Kolesnikov, Dirk Weissenborn, Xiaohua Zhai, Thomas Unterthiner, Mostafa Dehghani, Matthias Minderer, Georg Heigold, Sylvain Gelly, Jakob Uszkoreit, and Neil Houlsby. An image is worth 16x16 words: Transformers for image recognition at scale. In *International Conference on Learning Representations*, 2021. 3
- [16] Ariel Ephrat, Inbar Mosseri, Oran Lang, Tali Dekel, Kevin Wilson, Avinatan Hassidim, William T Freeman, and Michael Rubinstein. Looking to listen at the cocktail party: A speaker-independent audio-visual model for speech separation. *ACM Transactions on Graphics*, 37(4):1–11, 2018. 2
- [17] Souheil Fenghour, Daqing Chen, Kun Guo, and Perry Xiao. Lip reading sentences using deep learning with only visual cues. *IEEE Access*, 8:215516–215530, 2020. 3
- [18] John N Gowdy, Amarnag Subramanya, Chris Bartels, and Jeff Bilmes. Dbn based multi-stream models for audio-visual speech recognition. In *2004 IEEE International conference on acoustics, speech, and signal processing*, volume 1, pages I–993. IEEE, 2004. 2
- [19] Anmol Gulati, James Qin, Chung-Cheng Chiu, Niki Parmar, Yu Zhang, Jiahui Yu, Wei Han, Shibo Wang, Zhengdong Zhang, Yonghui Wu, and Ruoming Pang. Conformer: Convolution-augmented transformer for speech recognition. In *INTERSPEECH*, 2020. 2
- [20] Saumya Jetley, Nicholas A Lord, Namhoon Lee, and Philip HS Torr. Learn to pay attention. In *Proc. ICLR*, 2018. 3
- [21] Abhishek Jha, Vinay Namboodiri, and C. Jawahar. Spotting words in silent speech videos: a retrieval-based approach. *Machine Vision and Applications*, 30, 03 2019. 1
- [22] Benjamin Johnston and Philip Chazal. A review of image-based automatic facial landmark identification techniques. *EURASIP Journal on Image and Video Processing*, 2018:86, 09 2018. 1
- [23] Anjuli Kannan, Yonghui Wu, Patrick Nguyen, Tara N. Sainath, Zhifeng Chen, and Rohit Prabhavalkar. An analysis of incorporating an external language model into a sequence-to-sequence model. In *Proc. ICASSP*, 2018. 3
- [24] Angelos Katharopoulos, Apoorv Vyas, Nikolaos Pappas, and François Fleuret. Transformers are rnns: Fast autoregressive transformers with linear attention. In *International Conference on Machine Learning*, pages 5156–5165. PMLR, 2020. 5
- [25] Diederik P. Kingma and Max Welling. Auto-encoding variational bayes. In *Proc. ICLR*, 2014. 6
- [26] Oscar Koller, Hermann Ney, and Richard Bowden. Deep learning of mouth shapes for sign language. In *2015 IEEE International Conference on Computer Vision Workshop (ICCVW)*, pages 477–483, 2015. 3
- [27] Alexandros Koumparoulis, Gerasimos Potamianos, Youssef Mroueh, and Steven J. Rennie. Exploring roi size in deep learning based lipreading. In *Proc. The 14th International Conference on Auditory-Visual Speech Processing*, pages 64–69, 2017. 3
- [28] Wei Li, Sicheng Wang, Ming Lei, Sabato Marco Siniscalchi, and Chin-Hui Lee. Improving audio-visual speech recognition performance with cross-modal student-teacher training. In *Proc. ICASSP*, pages 6560–6564. IEEE, 2019. 2
- [29] Karen Livescu, Ozgur Cetin, Mark Hasegawa-Johnson, Simon King, Chris Bartels, Nash Borges, Arthur Kantor, Partha Lal, Lisa Yung, Ari Bezman, et al. Articulatory feature-based methods for acoustic and audio-visual speech recognition: Summary from the 2006 jhu summer workshop. In *2007 IEEE International Conference on Acoustics, Speech and Signal Processing-ICASSP'07*, volume 4, pages IV–621. IEEE, 2007. 2
- [30] Pingchuan Ma, Stavros Petridis, and Maja Pantic. End-to-end audio-visual speech recognition with conformers. In *ICASSP*, 2021. 3, 6
- [31] Andrew L. Maas, Ziang Xie, Dan Jurafsky, and Andrew Y. Ng. Lexicon-free conversational speech recognition with neural networks. In *Proceedings the North American Chapter of the Association for Computational Linguistics*, 2015. 3
- [32] Takaki Makino, Hank Liao, Yannis Assael, Brendan Shillingford, Basilio Garcia, Otavio Braga, and Olivier Siohan. Recurrent neural network transducer for audio-visual speech recognition. In *IEEE Workshop on Automatic Speech Recognition and Understanding*, 2019. 2, 3, 6, 7, 8
- [33] Michael McAuliffe, Michaela Socolof, Sarah Mihuc, M. Wagner, and Morgan Sonderegger. Montreal forced aligner: Trainable text-speech alignment using kald. In *INTERSPEECH*, 2017. 5
- [34] Liliane Momeni, Triantafyllos Afouras, Themis Stafylakis, Samuel Albanie, and Andrew Zisserman. Seeing wake words: Audio-visual keyword spotting. In *Proc. BMVC*, 2020. 2
- [35] Eng-Jon Ong and Richard Bowden. Learning temporal signatures for lip reading. In *2011 IEEE International Conference on Computer Vision Workshops (ICCV Workshops)*, pages 958–965, 2011. 2
- [36] George Papandreou, Athanassios Katsamanis, Vassilis Pitsikalis, and Petros Maragos. Adaptive multimodal fusion by uncertainty compensation with application to audiovisual speech recognition. *Audio, Speech, and Language Processing, IEEE Transactions on*, 17(3):423–435, 2009. 2
- [37] Stavros Petridis, Themis Stafylakis, Pingchuan Ma, Feipeng Cai, Georgios Tzimiropoulos, and Maja Pantic. End-to-end audiovisual speech recognition. *CoRR*, abs/1802.06424, 2018. 3
- [38] Stavros Petridis, Themis Stafylakis, Pingchuan Ma, Georgios Tzimiropoulos, and Maja Pantic. Audio-Visual Speech Recognition with a Hybrid CTC/Attention Architecture. In *IEEE Spoken Language Technology Workshop*, pages 513–520, 2018. 2, 3, 5, 6
- [39] G. Potamianos, C. Neti, G. Gravier, A. Garg, and A.W. Senior. Recent advances in the automatic recognition of audio-visual speech. *Proceedings of the IEEE*, 91(9):1306–1326, 2003. 2

- [40] Alec Radford, Jeffrey Wu, Rewon Child, David Luan, Dario Amodei, Ilya Sutskever, et al. Language models are unsupervised multitask learners. *OpenAI blog*, 1(8):9, 2019. 4
- [41] Brendan Shillingford, Yannis Assael, Matthew W. Hoffman, Thomas Paine, Cian Hughes, Utsav Prabhu, Hank Liao, Hasim Sak, Kanishka Rao, Lorraine Bennett, Marie Mulville, Ben Coppin, Ben Laurie, Andrew Senior, and Nando de Freitas. Large-Scale Visual Speech Recognition. In *INTERSPEECH*, 2019. 1, 2, 3, 6, 8
- [42] Themis Stafylakis and Georgios Tzimiropoulos. Combining residual networks with lstms for lipreading. In *Interspeech*, 2017. 2, 3
- [43] Gül Varol, Liliane Momeni, Samuel Albanie, Triantafyllos Afouras, and Andrew Zisserman. Read and attend: Temporal localisation in sign language videos. In *Proc. CVPR*, 2021. 2
- [44] Ashish Vaswani, Noam Shazeer, Niki Parmar, Jakob Uszkoreit, Llion Jones, Aidan N. Gomez, Lukasz Kaiser, and Illia Polosukhin. Attention Is All You Need. In *NeurIPS*, 2017. 3, 4, 5, 6
- [45] Xiaolong Wang, Ross Girshick, Abhinav Gupta, and Kaiming He. Non-local neural networks. In *Proc. CVPR*, pages 7794–7803, 2018. 3
- [46] Bichen Wu, Chenfeng Xu, Xiaoliang Dai, Alvin Wan, Peizhao Zhang, Masayoshi Tomizuka, Kurt Keutzer, and Peter Vajda. Visual transformers: Token-based image representation and processing for computer vision. *CoRR*, abs/2006.03677, 2020. 3
- [47] Yonghui Wu, Mike Schuster, Zhifeng Chen, Quoc V. Le, Mohammad Norouzi, Wolfgang Macherey, Maxim Krikun, Yuan Cao, Qin Gao, Klaus Macherey, Jeff Klingner, Apurva Shah, Melvin Johnson, Xiaobing Liu, Lukasz Kaiser, Stephan Gouws, Yoshikiyo Kato, Taku Kudo, Hideto Kazawa, Keith Stevens, George Kurian, Nishant Patil, Wei Wang, Cliff Young, Jason Smith, Jason Riesa, Alex Rudnick, Oriol Vinyals, Greg Corrado, Macduff Hughes, and Jeffrey Dean. Google’s neural machine translation system: Bridging the gap between human and machine translation. *CoRR*, abs/1609.08144, 2016. 4
- [48] Zhuyu Yao, Jiangbo Ai, Boxun Li, and Chi Zhang. Efficient DETR: improving end-to-end object detector with dense prior. *CoRR*, abs/2104.01318, 2021. 3
- [49] Jianwei Yu, Shi-Xiong Zhang, Jian Wu, Shahram Ghorbani, Bo Wu, Shiyin Kang, Shansong Liu, Xunying Liu, Helen Meng, and Dong Yu. Audio-visual recognition of overlapped speech for the lrs2 dataset. In *ICASSP*, pages 6984–6988, 05 2020. 2, 6
- [50] Yuhui Yuan and Jingdong Wang. Ocnet: Object context network for scene parsing. In *arXiv preprint arXiv:1809.00916*, 2018. 3
- [51] Xingxuan Zhang, Feng Cheng, and Shilin Wang. Spatio-temporal fusion based convolutional sequence learning for lip reading. In *Proc. ICCV*, pages 713–722, 2019. 2, 3, 6
- [52] Yuanhang Zhang, Shuang Yang, Jingyun Xiao, Shiguang Shan, and Xilin Chen. Can We Read Speech Beyond the Lips? Rethinking RoI Selection for Deep Visual Speech Recognition. In *arXiv preprint arXiv:2003.03206*, 2020. 2, 3
- [53] Ya Zhao, Rui Xu, Xinchao Wang, Peng Hou, Haihong Tang, and Mingli Song. Hearing lips: Improving lip reading by distilling speech recognizers. In *arXiv preprint arXiv:1911.11502*, 2019. 6
- [54] Ziheng Zhou, Guoying Zhao, Xiaopeng Hong, and Matti Pietikäinen. A review of recent advances in visual speech decoding. *Image and vision computing*, 32(9):590–605, 2014. 2